

ACTMINER: Applying Causality Tracking and Increment Aligning for Graph-based Threat Hunting

Mingjun Ma, Tiantian Zhu*, Tieming Chen, Shuang Li, Jie Ying, Aohan Zheng, Chunlin Xiong, Mingqi Lv, and Yan Chen, IEEE Fellow

Abstract—To defend against Advanced Persistent Threats on the endpoint, threat hunting employs security knowledge such as cyber threat intelligence to continuously analyze system audit logs through retrospective scanning, querying, or pattern matching, aiming to uncover attack patterns/graphs that traditional detection methods (e.g., recognition for Point of Interest) fail to capture. However, existing threat hunting systems based on provenance graphs face challenges of high false negatives, high false positives, and low efficiency when confronted with diverse attack tactics and voluminous audit logs.

To address these issues, we propose a system called ACTMINER, which constructs query graphs from descriptive relationships in cyber threat intelligence reports for precise threat hunting (i.e., graph alignment) on provenance graphs. First, we present a heuristic search strategy based on equivalent semantic transfer to reduce false negatives. Second, we establish a filtering mechanism based on causal relationships of attack behaviors to mitigate false positives. Finally, we design a tree structure to incrementally update the alignment results, significantly improving hunting efficiency. Evaluation on the DARPA Engagement dataset demonstrates that compared to the SOTA POIROT, ACTMINER reduces false positives by 39.1%, eliminates all false negatives, and effectively counters adversarial attacks.

Index Terms—Threat Hunting, Advanced Persistent Threat, Attack Scenario Graph, Data Provenance.

I. INTRODUCTION

Advanced Persistent Threats (APTs) aim to infiltrate specific institutions to obtain critical asset information and sensitive data, posing immense threats and impacts. In order to detect and investigate APT attacks on hosts, data provenance [1] is widely used to analyze basic events (e.g., a sensitive file written by a malicious process) step-by-step. Nowadays, there are increasingly researchers have begun to employ provenance graphs in the field of APT attack detection on hosts.

Existing provenance-based systems for detecting APTs fall into the following two main categories: rule-based [2]–[10],

This work is supported by the following grants: National Natural Science Foundation of China under Grant No. U22B2028 and 62372410. The Fundamental Research Funds for the Provincial Universities of Zhejiang under Grant No. RF-A2023009. Zhejiang Provincial Natural Science Foundation of China under Grant No. LZ23F020011.

M. Ma, T. Zhu, T. Chen, S. Li, J. Ying, Q. Yuan and M. Lv are with the College of Computer Science and Technology, Zhejiang University of Technology, Hangzhou 310023, China. E-mail: zjutmmj@zjut.edu.cn, ttzhu@zjut.edu.cn*, tmchen@zjut.edu.cn, lish@zjut.edu.cn, jieying@zjut.edu.cn, zjutzah@zjut.edu.cn, mingqilv@zjut.edu.cn. *corresponding author

C. Xiong is with the China Unicom (Guangdong) Industrial Internet Co., Ltd., Guangzhou 510555, China. E-mail: chunlinxiong@gmail.com.

Y. Chen is with Department of Electrical Engineering and Computer Science, Northwestern University, Evanston, IL 60208, USA. E-mail: ychen@northwestern.edu.

and learning-based [11]–[17]. The policies presented by rule-based systems are difficult to sustain in a constantly changing system environment, analysts must frequently update the rule base to adapt to new types of attacks, and the lag in defense results in frequent occurrences of false negatives. From the perspective of detection granularity, learning-based detection methods can be categorized into graph-level [11], [14], [15], [17], node/edge-level [12], [13], [16]. Graph-level detection typically involves learning the characteristics of benign graphs and use certain technique like clustering to discern abnormal ones. However, in the anomalous subgraph [14], [15], [17], not all nodes/edges are necessarily associated with the attack. Experts still need further analysis to pinpoint the malicious attack path accurately. In contrast, node/edge-level detection methods are able to obtain the point of interesting (POI), which makes it more direct and effective than graph-level ones in locating the attack candidate. However, the alerts that solely focus on nodes and edges do not fully reveal the panorama of the attack, and analysts still need to spend a significant amount of time evaluating whether the generated POIs are false positives [12], [13], [16]. According to CrowdStrike’s 2024 Global Threat Report [18], the time to compromise a host has gone from 84 minutes in 2022 to 62 minutes in 2023. This means that if an attack is not detected and responded to in a timely manner, the attacker will likely have a lateral movement [19] that will cause more hazards.

Considering the shortcomings of the above detection systems, POIROT [2] has proposed a threat hunting approach based on graph alignment. It extracts the query graph from Cyber threat intelligence reports and then performs graph matching on the provenance graph to capture malicious behaviors. Due to the inherent interpretability of the query graph, its matching results can reflect comprehensive information about the attack, enabling analysts to respond accurately and promptly to the attack.

But POIROT still faces the following three limitations:

- **Semantic Gap (C1)**. How to apply the attack knowledge extracted from CTI reports to solve the problems of attack camouflage and persistence. The extracted query graphs are often difficult to be directly mapped one-to-one to the provenance graph (e.g., files with the same type but different names). These mismatches between the two graphs can lead to inaccurate detection outcomes.

- **Temporal & Causality Missing (C2)**. How to detect causal relationships of attacks in dynamic scenarios to minimize erroneous alerts. Solely concentrating on a single behavior can overwhelm the hunting system with an influx

of alerts, thereby hindering its ability to effectively identify and mitigate truly malicious activities (e.g., discerning the semantic differences in the access to sensitive files such as `/etc/passwd` between normal processes and malicious processes requires consideration of causal relationships). This disregard may lead to more imprecise detection, rendering the system ineffective in countering sophisticated threats.

- **Data explosion Dilemmas (C3)**. How to minimize memory overhead and enhance the efficiency of threat hunting. Existing solutions assume an ideal scenario for datasets, that is, researchers assume that a complete attack can be discovered within a single batch of data. However, APT exhibits persistence, and attack chains may span across different batches of data (e.g., data from the first and third days). Repeated scans on ever-expanding datasets introduce significant overhead.

In this work, we propose ACTMINER, a threat hunting system that combines causality tracking and incremental aligning to efficiently and accurately dig attack chains. **To tackle C1**, ACTMINER constructs a heuristic search strategy based on equivalent semantic transfer to counter phenomena such as attack camouflage, persistence, and evasion. We fuse the data information of inter-entity interactions through entities and their contextual semantics in order to achieve the accurate capture of malicious behaviors. **To address C2**, ACTMINER constructs a filtering mechanism based on the causal relationships of attack behaviors, and ignores unreasonable entity context relationships. ACTMINER employs the causal motivation behind attacks to guide threat hunting, ensuring the interpretability of hunting results and minimizing false positives. In other words, we provide a more accurate hunting result by excluding unreasonable (attack-irrelevant) paths based on the causal relationship through temporal sequences. **To deal with C3**, ACTMINER constructs a tree structure to incrementally update the alignment results, thereby avoiding the significant overhead caused by rescanning multiple batches of redundant data.

We evaluate the effectiveness and efficiency of ACTMINER on the dataset provided by Darpa TC program [20], [21]. Our results reveal that ACTMINER surpasses existing provenance-based threat hunting system in terms of detection precision and recall. Moreover, ACTMINER can reduce the computational overhead and eliminate redundant searches. By deploying ACTMINER, security analysts are able to effectively analyze attack chains and formulate countermeasures, significantly alleviating the workload. In summary, the main contributions of our work are as follows:

- Unlike traditional attack detection methods, we propose a provenance-based threat hunting system ACTMINER to accurately capture attack chains.
- We introduce a heuristic search strategy based on equivalent semantic transfer and a filtering mechanism based on causal relationships of attack behaviors to ensure the precision and recall of ACTMINER.
- We propose a tree structure to incrementally update the alignment results, effectively addressing persistent APT attacks and the continuous growth of graph data.
- We comprehensively evaluate our system and SOTA POIROT [2] on the dataset from DARPA TC program.

The results demonstrate the efficiency of ACTMINER in capturing the attack chain and highlight its resistance to adversarial attacks.

II. BACKGROUND KNOWLEDGE

A. Provenance Graph

Provenance graphs possess potent semantic expressiveness and contextual association capabilities, embodying the concrete manifestation of kernel audit logs. They model all system entities within the logs as nodes and the interactions between entities as edges, where both nodes and edges bear attribute information. The nodes within the provenance graph are categorized into subjects and objects based on the direction of data movement. Edges represent the causal relationships between system entities, such as read/write file operations, execute executable file operations, create/clone process operations, and so forth. By leveraging provenance graphs, security professionals can associate malicious entities with attack behaviors through causal analysis, unveiling the complete picture of an attack.

B. CTI Report and Query Graph

Cyber threat intelligence (CTI) reports [22]–[24] encompass comprehensive information related to cyber attacks and attackers, with a particular emphasis on capturing detailed attack procedures - the intricate sequences of steps and techniques employed in multi-stage attacks. These reports provide in-depth representations of attack scenarios, potential impacts on target hosts, as well as the complex chains of causally-linked events that characterize APTs. Security professionals leverage CTI reports to formulate more targeted defense rules for preventing and identifying malicious attack behaviors. In recent years, substantial research [2], [11], [25]–[27], has demonstrated the successful application of CTI reports in threat detection and threat hunting. In this paper, we construct a directed graph, termed the query graph, from the offensive and defensive knowledge [28] (attack entities and their causal relationships) extracted from CTI reports. Similar to provenance graphs, query graphs are directed graphs with attribute information.

C. Graph Alignment

Graph alignment refers to the problem of detecting potential cyber intrusion behaviors by establishing an optimal subgraph mapping between a provenance graph (G_p) representing system activities across the entire system, and a query graph (G_q) representing attack pattern activities. The provenance graph $G_p = (V_p, E_p)$ consists of a node set V_p representing system entities and events, and an edge set E_p . The query graph $G_q = (V_q, E_q)$ comprises a node set V_q representing attack patterns and an edge set E_q . The goal of graph alignment is to find a subgraph G_m in G_p that maximizes the matching degree with G_q :

$$G_m = \operatorname{argmax}_{G' \subseteq G_p} (M(G', G_q)) \quad (1)$$

Here, M is the Matches function that calculates the matching degree between G_q and a subgraph G' of G_p . By solving this optimization problem, the best mapping from the attack query graph to the activity graph is obtained, enabling the detection and tracking of cyber intrusion behaviors.

III. MOTIVATION

A. Motivating Example

Scenario: Consider the following scenario where an attacker exploits the feature of automatically executing login scripts (Reg.exe and %temp% \art.bat_2) during login initialization (mal) to establish persistence by adding the malicious script path to the registry (HKCU \Environment_R2). Subsequently, the attacker searches for network shares on the compromised computer to locate files and then collects sensitive data (/etc/passwd) from remote locations via shared network drives (host shared directories, network file servers, etc.). Finally, the data is transmitted over the network (162.66.239.75).

As illustrated in Figure 1, this example includes two graphs: the top-left depicts the attack query graph manually extracted from a cyber threat intelligence (CTI) report, following the approach outlined in the POIROT.

The attack initiates by leveraging a malicious executable, malicious.exe, to obtain unauthorized system access. It then employs Registry modifications to establish persistence. Once a foothold is secured, the attacker can remotely issue commands and execute them on the system, executing an *art.bat_2* file in the temporary folder and facilitating actions such as exfiltrating sensitive data to an external IP, exemplified by the transfer of /etc/passwd containing user account information.

On the right side is the provenance graph constructed from actual system logs capturing the observed execution behavior. Due to the fragmented nature of attack scenarios, coupled with the constraint of limiting the hop count to existing threat hunting approaches, can lead to imprecise or incomplete results during the threat hunting process. In this paper, we transform the threat-hunting problem into finding the attack query graph within the provenance graph.

Threat hunting methods centered around POIROT encounter several significant challenges:

False Negative. Due to the complexity of real enterprise environments, semantic gaps exist between provenance graphs and attack query graphs. The manifestations of the same attack type may differ across systems, and attackers may utilize the same tools in diverse ways. For instance, entity names in the attack query graph may have varying representations in the underlying logs of different systems. In POIROT, regular expressions are employed to instantiate node names from the attack query graph for hunting searches in the provenance graph. However, if attackers modify their tactics, introducing technical variations, threat hunting systems struggle to detect different mutated attack samples (e.g., over 100 versions of the Carbanak malware were described in CTI reports). Furthermore, attackers can evade security detection through obfuscation, persistence, and evasion techniques. As illustrated, the attack query graph only describes data exfiltration over the network, whereas in the real environment, the attacker creates

processes to read files, followed by another process reading those files, and finally transmitting them over the network. Overreliance on the simplistic approach of threat hunting based on a predetermined number of hops may inadvertently overlook malicious activities that align with the intrinsic characteristics of attacks, ultimately resulting in detection efforts failure. As shown in Figure 1, in a simulated scenario, as described in [2] Section 5, we set C_{thr} to 3, but find that this limitation resulted in an incomplete capture of the attack chain. Consequently, it was unable to detect the *art.bat* file. Moreover, with such hop count restrictions, attackers aware of the imposed limits could potentially evade hunting more easily across different scenarios, resulting in potential harm. The manual adjustment of the hop limit according to different scenarios poses significant challenges. Similarly, the same problem exists in other path-based detection [29]–[31] efforts.

False Positive. Within real organizations, extensive legitimate user operations exhibit similarities with attack behaviors in log data. If hunting rules are overly broad or incomplete, normal behaviors may be misclassified as malicious. For example, when a user downloads network files through a browser, the browser collects user data and transmits it to its cloud server, while the downloaded network files may be flagged as "suspicious files" by the system, resembling malicious attack behaviors and triggering false alarms from the hunting system. Additionally, attackers may leverage tools/techniques to deceive hunting systems, also leading to false positives. As highlighted in Figure 1, a suspicious process *Mal.exe* exhibits two paths for reading/writing sensitive files. According to the attack query graph, sensitive file access should occur before network transmission, while $path_1$ occurs after transmission. Therefore, $path_2$ represents the attacker's actual operations in the environment.

High overhead and inefficiency. Government and enterprise organizations typically need to collect data simultaneously from thousands of machines, easily amassing petabyte-scale data volumes. This massive data not only imposes substantial storage overhead but also significantly reduces hunting efficiency. Traditional hunting methods require offline storage and continuous backscanning of system log data, resulting in immense computational overhead for each hunting operation. Referring to Figure 1, assume that all operations before node *E23.txt* at time 114 have already occurred. When a security analyst attempts to hunt for threats solely based on the data collected after this time, the incremental data segment alone cannot effectively support the reconstruction of the complete attack chain represented by its query graph. When examining the issue holistically, the newly acquired data lacks the necessary evidence to capture the earlier stages of the multi-step intrusion. Consequently, subsequent data collection would necessitate rescanning the previously available information, redundantly recomputing the provenance of data prior to a specific timeframe. These redundant computations across multiple hunting activities introduce an unsustainable overhead, hindering the system's efficiency and scalability. And potentially allowing malicious activities to persist undetected for extended periods.

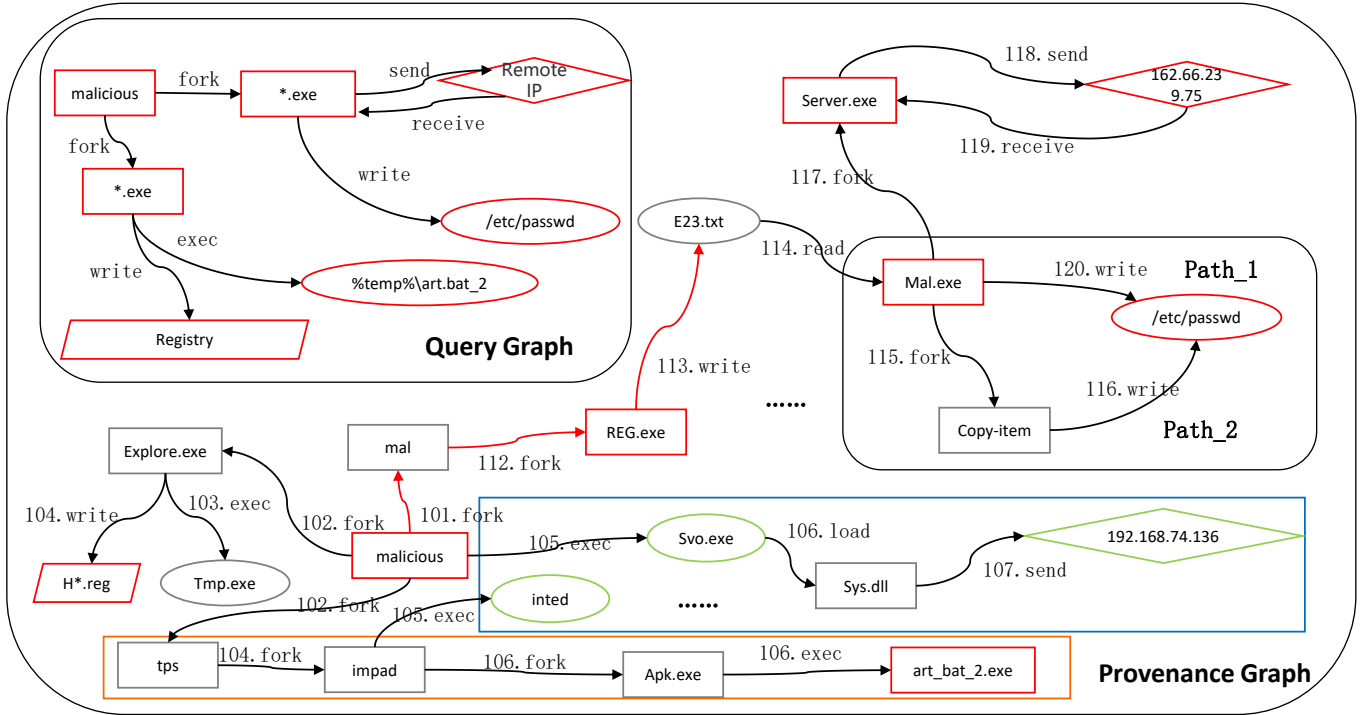


Fig. 1: Motivating Example. The red nodes and edges depict the truly malicious behavior. In contrast, the blue outlines encompass false positive detection, where POIROT incorrectly identified benign system entities as malicious. The specific nodes are the points with green borders. Furthermore, the orange outlines highlight the instances of missed detection or false negatives, where POIROT failed to identify nodes that were indeed part of the attack chain.

IV. SYSTEM DESIGN

This section first introduces the overall architecture of the ACTMINER system, followed by a detailed description of each module presented in ACTMINER.

A. System Overview

Data Preparation Module (§ IV-B). The attack query graphs are extracted from threat intelligence reports, and provenance graphs are constructed based on extensive underlying logs. Duplicate events and orphan nodes within the provenance graphs undergo filtering, which is a necessary and common practice in existing work [32].

Casual Relation and Semantic Processing Module (§ IV-C). When a new attack query graph or provenance graph generated, ACTMINER will first categorize the entities into four classes. Then the provenance graph will delivery to the next module while the attack query graph still need to be processed. Next, ACTMINER merges analogous actions in the attack query graph. Finally, ACTMINER employs *Equivalent Semantic Transfer* which traces potentially overlooked attack chains by tracking malicious semantics, to identify the suspicious actions in the next module.

Threat Hunting and Incremental Aligning Module (§ IV-D). ACTMINER will hunt attack-related scenario by chaining suspicious semantic nodes and generating suspicious semantic tree. As time progresses, batch data is continuously inputted into the ACTMINER, persistently updating our suspicious semantic trees and unveiling more latent malicious

attacks. And to control the memory consumption, ACTMINER will store the unupdated tree branch to the database unless certain behavior related to this branch.

The basic architecture of ACTMINER is shown in Figure 2, which can be divided into three modules: (I) the Data Preparation Module, (II) Casual Relation and Semantic Processing Module, and (III) Threat Hunting and Incremental Aligning Module. It is important to note that ACTMINER continuously runs the above three modules as the time progresses. Details of system design for each module are given in Section IV-B, Section IV-C, Section IV-D, respectively.

B. Data Preparation Module

This section describes the data preprocessing module for provenance graphs and query graphs.

1) *Provenance Preparation*: Provenance graphs are composed of log data collected from various platforms by data collectors. In this work, we employ open-source tools such as eAuditd [33], Kollect [34], and Event Tracing for Windows (ETW) [35] to gather relevant system logs from Linux and Windows environments. ACTMINER transforms each event into a directed, time-stamped edge, in which the source node represents the object being acted upon. For any event $et \in E$, ACTMINER represents it as a quintuple $\langle UID_s, UID_o, OP, T_i \rangle$. UID_s and UID_o are unique identifiers for the subject and object of et , respectively. OP denotes the type of et , and T_i denotes the time when et occurred.

Directly processing such massive raw log data is extremely challenging. To address this, we perform pruning operations on

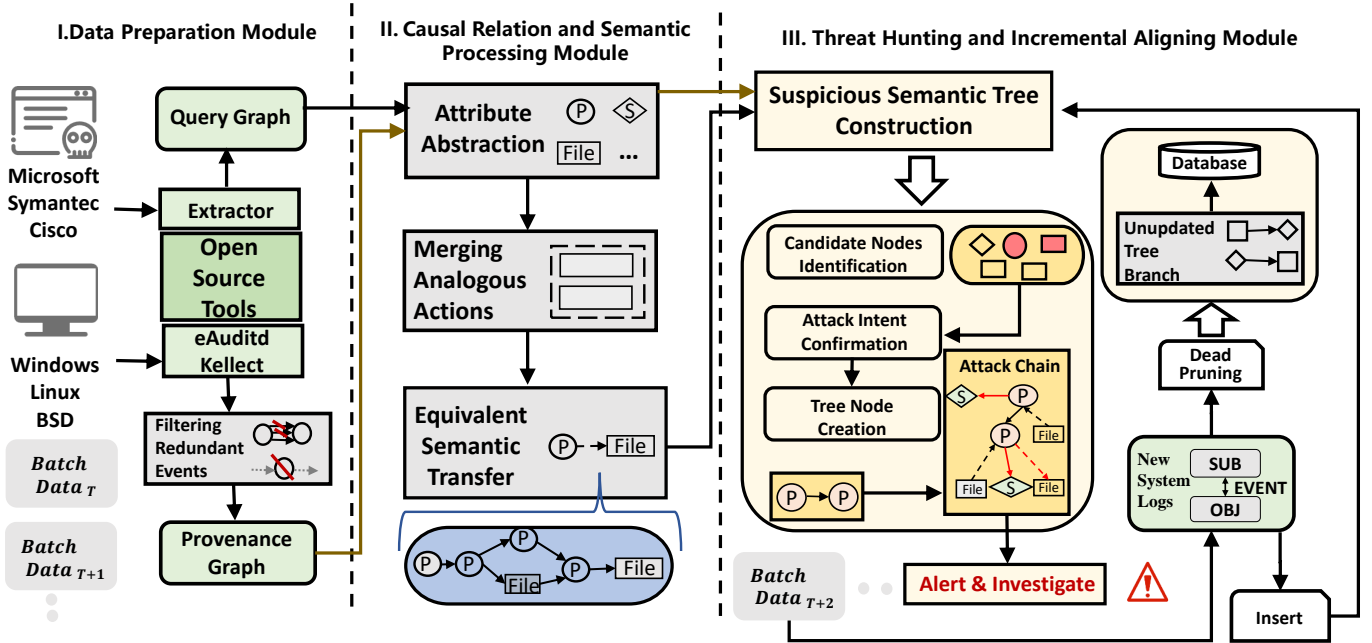


Fig. 2: The architecture of ACTMINER, which consists of three core modules that synergistically facilitate comprehensive threat hunting and attack chain construction capabilities.

the low-level log data. Specifically, redundant events without context are removed [9], [36]. This means if the subject UID (UID_s), object UID (UID_o), and operation (OP) are identical, and the timestamps (T_i) are consecutive, the most recent timestamp will be preserved. Furthermore, our methodology includes the removal of isolated nodes within the provenance graph. The isolated nodes refer to entities that lack any incoming or outgoing edges. For example, we find that the data contains many these nodes manifest without any parent or child nodes, none of the events contain a subject UID (UID_s) or object UID (UID_o) matching the UID of the node, lack contextual information and fail to provide meaningful insights. So remove them do not compromise the integrity of the graph representation.

Concurrently, during the process of constructing provenance graphs, the node types are categorized based on the entity type contained within the logs. For instance, F_a represents files involving user and system-sensitive information, such as the boot.ini file on Windows and /etc/passwd file on Linux. The specific categorization is detailed in Table I.

As show in Table I, we are inspired by APTShield [9], Conan [8] and refined the classification heuristics optimized the classification method we obtained from POIROT. Furthermore, we extensively gather CTI reports from various online sources and network channels, identifying specific file paths that exhibit heightened susceptibility to attacks. Consequently, we adapt the importance degree of these paths based on their frequency of occurrence to finally obtain ten distinct labels.

By analyzing the CDM18 and CDM19 which refer to the data definitions for DARPA's E3 and E4 programs, respectively, we adopt events based on a few general fields in the CDM (i.e., the events of read, write, fork, clone, create, execute, load, and inject), which were most commonly used

TABLE I: A categorization of distinct entities and their corresponding label assignments.

Entity	Tag	Description
Process	P	Processes, threads spawned by system calls
User Configuration Sensitive Files	Fa	Sensitive files containing user configuration information, such as /etc/passwd
Application Configuration Sensitive Files	Fb	Sensitive files that contain configuration information about the application, such as /etc/mysql/my.cnf
Log-sensitive documents	Fc	Sensitive files containing logging information, e.g. /etc/httpd/logs, e.g. /etc/httpd/logs
Library file	Fd	A collection of pre-compiled methods with extensions such as .lib, .a, .dll, .so, etc.
Executable file	Fe	Files that can be loaded and executed by the operating system, with extensions such as: .exe, .vbs, etc.
Temporary document	Ff	Temporary files generated by the system, e.g., /tmp/*
Other documents	Fg	A collection of other types of files, such as plain text files, plain graph files, plain zip files, etc.
Registration form	R	Unified management of hardware and software configurations, including HKLM, HKCU, HKCR, HKCC, HKU, etc.
Socket	S	Refers to a host on the Internet or a process in a host, e.g. 127.0.0.1

in previous studies such as Holme [3], Sleuth [10], and Morse [4]. The details are show in Table II.

2) *Query Graph Preparation.*: CTI reports describe attacks that have already occurred. We collect the latest threat intelligence from websites such as Microsoft and Symantec. Leveraging open-source tools like Extractor [28], we extract attack query graphs (G_q) from cyber threat intelligence (CTI) reports. Analogous to provenance graphs, upon extracting attack query graphs, the constituent entities undergo a corresponding mapping process.

C. Casual Relation and Semantic Processing Module

In this section, we sequentially describe the process of Module II in Figure 2, i.e., merging analogous actions and equivalent semantic transfer. In a nutshell, analogous actions in attack query graphs are merged while employing an equivalent semantic transfer strategy. This process enhances attack

TABLE II: Classification of different event types.

Number	EventType	Subject	Object	Direction	Description
1	accept	P	S	backward	Accepting socket connections
2	inject	P	P	forward	Running arbitrary code in the address space of independent activity processes.
3	clone	P	P	forward	Cloned subject
4	connect	P	S	forward	Connect to a socket type guest
5	execute	P	F	forward	The subject invokes and executes the object
6	fork	P	P	forward	Creating the process body
7	load	P	F	backward	Load file to current workspace data
8	write	P	F	forward	Open a file or directory (Object) and write information
9	receive	P	S	backward	Receive data through a connected socket port
10	send	P	S	forward	Sending data through a connected socket port
11	exit	P	P	forward	Process exit
12	unlink	P	F	forward	Deletion of individual files

hunting capabilities while simultaneously preparing the data for input to Module III.

1) *Merging Analogous Actions*: When ACTMINER adopts the attack query graphs to perform the threat hunting tasks, it encounters the issue of *rigid matching*. This situation leads the alignment between attack query graphs and provenance graphs become hard to achieve. Finally, it would result in high false negative and positive rate in the Module III.

Additionally, the directly extracted G_q is fixed, which limits its ability to generalize and effectively defend against variants of known attacks, as it is specifically tailored to documented attack patterns. To address this challenge, there is a key insights of ACTMINER: *merging analogous actions*. This method integrates nodes with similar operations. For instance, instead of representing each individual file with a distinct node, the generalized G_q may group files based on their types (e.g., F_a, F_b, F_c in Table I) in the attack chain. Simultaneously, we consider the temporal relationships of attack events. Processes can be merged based on their functional attributes or the operations they perform, rather than being strictly tied to specific executable paths or process names. In essence, this method is to transform the information flow from the source entity to the same target entity while preserving the semantic meaning of the source entity, so that equivalent events can be removed as redundant information, thereby achieving efficient compression of the data.

2) *Equivalent Semantic Transfer*: During the attack process, malicious processes controlled by the attacker interact with other entities [8], causing malicious behaviors and effects to proliferate across the system through the intricate web of entity interactions and information propagation pathways, thereby expanding the attacker’s control scope.

Based on above finding, we construct the equivalent semantics transitivity strategy to address the false negative issue. The key insight of this strategy is that the semantics of malicious behavior propagate with taking actions. As shown in Figure 3.(a), it depicts a short attack path described in the query graph, where a process controlled by the attacker tampers with sensitive files. Figure 3.(b) illustrates one of the attacker’s specific implementation approaches: First, a process P1 with suspicious semantics injects malicious code to create process P2; then, process P2 writes a suspicious file Fe; next, another malicious process P3 accesses the tainted file; subsequently, the process P3 with suspicious semantics creates process P4;

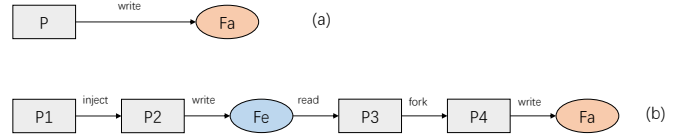


Fig. 3: An Example of equivalent semantic transitivity.

finally, process P4 with suspicious semantics performs a write operation on sensitive files. Through this series of operations, the ultimate behavior of a suspicious process tampering with sensitive files F_a is achieved. Although the types of controlled entities change during the attack process, the ultimate goal remains unchanged. The operations in (b) are essentially the same as (a) and align with the attacker’s intent, making the two paths semantically equivalent.

To comprehensively capture attack intents and mitigate attack evasion while addressing semantic gaps between G_q and G_p , we integrated log data from the DARPA project, leveraged attack stage theories proposed in previous works like Conan [8] and Aptshield [9], and incorporated relevant descriptions from the CDM document [37] to extract six equivalent semantic transitivity policies, as illustrated in Table III. Therefore, ACTMINER can track and locate suspicious behavior on the host in real-time by analyzing the data flow transmission, while systems like HOLMES [3] cannot do this (according to Table 8 in HOLMES). In contrast, Sleuth [10] can detect suspicious behavior in specific steps through initial label propagation, but its label propagation mechanism may fail if the attacker uses legitimate tools (such as the command line) to operate, and cannot accurately identify malicious intent. Based on the context information of entities, these policies automatically determine whether an event is attack-related. The subject represents a process, the object represents different types of entities connected with the subject, and the direction indicates the information flow between subject and object. For example, the third policy represents process \rightarrow file: if the process in the write event is considered attack-related, suspicious semantics will propagate from the process to the file. If another process reads the file containing suspicious semantics, the suspicious semantics will further propagate from the file to that process. Then, we use a heuristic search algorithm integrating equivalent semantic transitivity in

TABLE III: Equivalent Semantic Transitivity Policies in the Context of Generalized Attack Pattern Identification and Matching.

Subject	Object	Direction	Requisites
P	P	forward	$\exists p.\text{semantics}\{\text{SuspiciousLabel}\}$ $\wedge[\text{Event_Fork}(p, p') \mid \text{Event_Create}(p, p')]$ $\text{Event_Clone}(p, p'): p'.\text{semantics.add}(\text{"SuspiciousLabel"})$
P	P	forward	$\exists p.\text{semantics}\{\text{SuspiciousLabel}\}$ $\wedge\text{Event_Inject}(p, p'): p'.\text{semantics.add}(\text{"SuspiciousLabel"})$
P	F	forward	$\exists p.\text{semantics}\{\text{SuspiciousLabel}\}$ $\wedge\text{Event_Write}(p, f): f.\text{semantics.add}(\text{"SuspiciousLabel"})$ $\wedge\text{semantics}\{\text{SuspiciousLabel}\} \wedge \text{f.tag}\{\text{Fd, Fc}\}$
P	F	backward	$\exists f.\text{semantics}\{\text{SuspiciousLabel}\} \wedge \text{Event_Load}(p, f): p.\text{semantics.add}(\text{"SuspiciousLabel"})$
P	F	backward	$\exists f.\text{semantics}\{\text{SuspiciousLabel}\}$ $\wedge\text{Event_Read}(p, f): p.\text{semantics.add}(\text{"SuspiciousLabel"})$

Section IV-D.

D. Threat Hunting and Incremental Aligning Module

1) *Suspicious Semantic Tree Construction*: An event contains the interaction information between entities and can be transformed into an information flow, which can be further classified into data flows and control flows. Data flows indicate dependencies in data content, reflecting the data propagation path (e.g., a process reading a file), while control flows primarily refer to process creation relationships (e.g., a parent process creating a child process). In the threat hunting module, data flows and control flows will be jointly abstracted into a suspicious semantic tree. The process of generating a suspicious semantic tree is detailed as following three steps, as shown in algorithm 1:

Step 1: Finding Candidate Nodes. To capture malicious behaviors in the provenance graph constructed from low-level system logs that match the patterns in the corresponding query graph, our system first searches for all nodes in the provenance graph with attributes identical to those of entity node in the query graph. These candidate nodes are collected into a list, referred to as the candidate set $FC(i)$, which is associated with the query node (Line 7).

Step 2: Confirming Attack Intent. As the query graph G_q carries clear temporal features and causal relationships, we leverage these information to guide the attack detection reconstruction and reconstruction processes. This enables us to quickly determine the initial intrusion location, relevant entity nodes, and the sequence of attack events. Such a query graph can assist analysts in searching malicious behaviors effectively. The *ExtractRelevantNodes* function is subsequently invoked to identify the critical nodes within the query graph that are essential for comprehending the attack methodology (Line 8). This function operates by determining the next potential action nodes in G_p based on the preceding step F_c in G_q . The *ReconstructAttackSequence* algorithm reconstructs the attack sequence (Line 9), carefully aligning with the temporal and causal patterns within G_q . Unlike indiscriminate search methods, the approach is strategically guided by specific target nodes, precisely capturing the attacker's intended progression. The function determines the matching order by meticulously tracing the sequence of attacks delineated in the graph. ACTMINER evaluates whether nodes introduce malicious semantics, which is identified by first fixing the target nodes and then analyzing behavior within G_q . This process involves tracing actions from the fixed nodes to determine patterns indicating malicious intent, forming the basis for further analysis.

To optimize the traversal and analysis process, the algorithm stores context information for each node (Lines 11-15). This step avoids redundant traversals of the graph and enables the algorithm to order the edges based on timestamps, resulting in an ordered hunting sequence (Lines 16-19). This sequence is instrumental in guiding the subsequent steps of the algorithm. It will calculate the reciprocal of the length of the shortest path between nodes in G_q and G_p as the path score. For each node in G_q , the candidate node with the highest contribution value will be selected as the fixed node.

Step 3: Creating Tree Nodes. The final step of the algorithm involves the creation of tree nodes (Lines 19-27). Given the disparity in size between the query graph and the provenance graph, the *CreateTreeNode* function (Line 31) is utilized to map each query graph to one or more subgraphs in the provenance graph that exhibit similar patterns. The function specifically creates a branch in the tree for the attack entry point. This mapping is facilitated by the hunting sequence obtained in the previous step, enabling efficient detection navigation against the large and complex dataset.

After creating the tree nodes, when the attack progression exceeds the total attack sequence, the system raises an alert to notify security analysts of this anomalous situation.

To illustrate the aforementioned methodology, we present an example for better comprehension. We aim to find suspicious subgraphs similar to the query graph in the provenance graph shown in Figure 4. As observed, the representation above illustrates a concrete instantiation of the graph, whereas the depiction below presents an abstraction of the model. Assuming we start from the process P1 within the red box as the starting point of the attack chain (corresponds to the above is *powershell_1.exe*), according to the query graph, the next step should be to find an executable file associated with P1, with the edge semantics being a write event. In the graph, only the Fe1 node (corresponds to the above is *update.ps1*) satisfies this condition, so we can generate a tree node that stores a variety of data, including the unique identifier of the query graph, event type, and relevant temporal information to assist subsequent hunting tasks. This step is largely analogous for both approaches, with only marginal differences in storage efficiency and temporal performance, the detail can see in Section V-D.

Similarly, $P2$ will also be identified and generate a tree node (corresponds to the above is *powershell_2.exe*). However, when the flows in G_q come to be associated with the socket, multiple similar scenarios may arise. In the G_p , the path from P2 to the socket IP2 (indicated by the red arrow) satisfies the previously defined equivalent semantic transitivity policy, indicating that P2 and P3 share the same semantic information. Therefore, IP2 can be retained as a suspicious node, while generating a tree node and preserving the temporal relationship from P3 to IP2. But for the above scenario, the absence of the strategy and rigid aligning rules, a false positive result is produced. Likewise, the path from P2 to IP3 also satisfies the equivalent semantic transitivity policy (It is important to note that intermediate nodes will be represented in the form of equivalent semantic attributes within the initial P1 node's properties). However, for the path from P2 to IP1, although

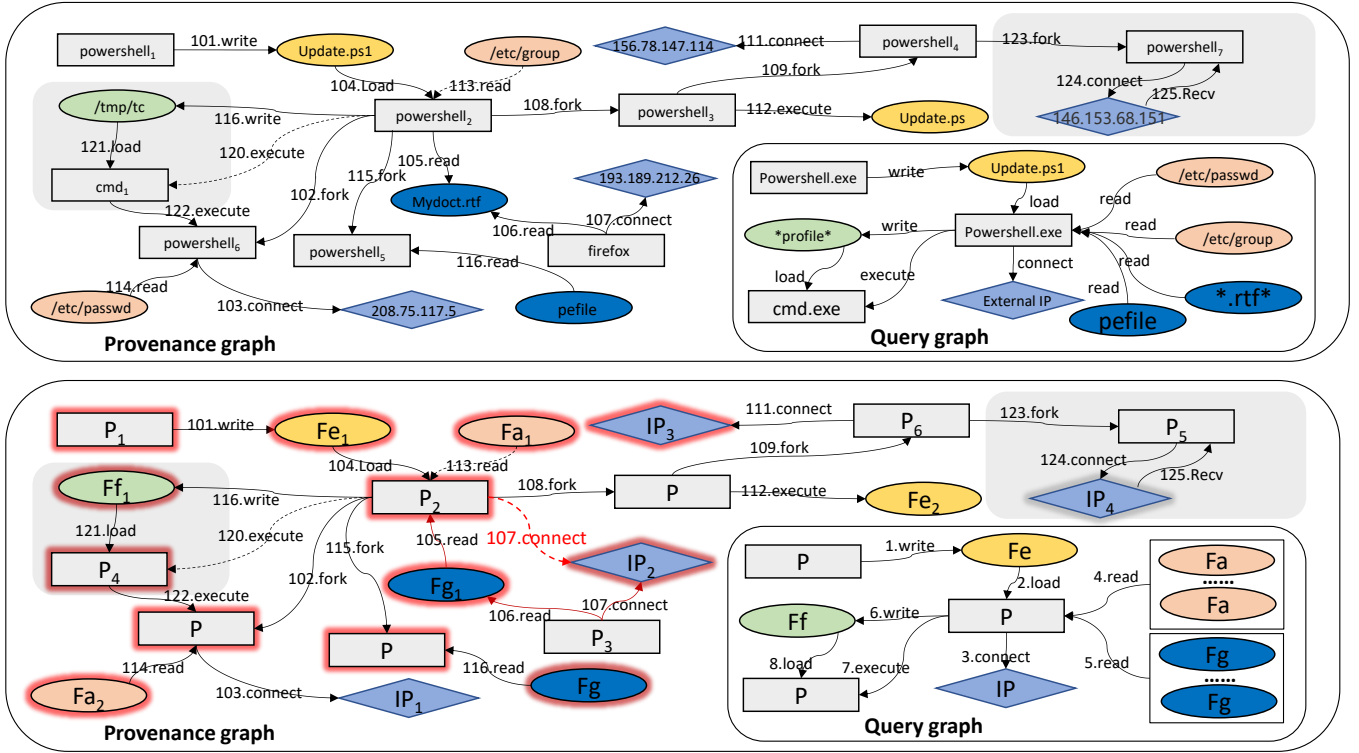


Fig. 4: A case study of strategies such as POIROT and the underlying scenarios that our ACTMINER faces in the same scenario. Where the dashed part indicates that the middle contains the multi-step behaviour whether black or red color, and the red line and red box part indicate the real captured entities and events.

it also represents $P \rightarrow IP$ with the edge semantics of a connect operation, it occurs before the previous node ($Fe_1 \rightarrow P_2$ at time 104), violating the sequence of the attack, and thus, this path is ignored. Fa can be found as the same.

Next, we need to find $P \rightarrow Ff$ (with the edge semantics of a write operation), but no files of the Ff type in the current provenance graph (assume the current time has not yet reached 116), so the system needs to wait for new data to arrive.

2) *Incremental Aligning*: As time progresses, the log data generated by hosts will continue to increase. For traditional threat hunting systems, for any newly added logs after a period of time, they need to re-scan the entire dataset with a larger volume. To address the inefficiency of traditional threat hunting in analyzing incremental streaming data, we adopt an incremental graph computation method to hunt for attacks and update suspicious semantic trees. First, we search for new candidate nodes in the newly arrived provenance graph based on the attributes of nodes in the query graph. Next, we divide the impact of the new data on the suspicious subtrees into two parts: the new data affects the existing suspicious semantic subtrees, and the new data is unrelated to the existing suspicious subtrees. Furthermore, to manage memory overhead effectively, we implement a forgetting rate to reduce memory consumption. We transfer the nodes that remain un-updated for a period of 6 hours (can be adjusted according to different circumstances) into the database and create a corresponding index for them. The index includes the attributes of the node itself and its parent node, enabling rapid localization of relevant nodes in the event of a subsequent occurrence. This

allows for the efficient retrieval and reinstatement of these nodes into memory.

For the former, through the affected tree nodes, we can obtain the current attack progress and their mapped nodes in the provenance graph and query graph. Then, through the sequence of suspicious candidate nodes, we can determine the next suspicious entity to hunt. Finally, we judge whether the suspicious states are met in the candidate node set of the suspicious entity, and if so, we construct a new tree node.

For the latter, we first determine whether the node has candidate nodes. If there are no candidate nodes, it means that this part of the data does not have an entry point for attacks, indicating that this part of the data is considered benign. However, if there are candidate nodes, we will start rebuilding the suspicious subtree from its candidate nodes.

As an example, the shaded part in Figure 4 represents the newly added data. For the new data, we determine whether it affects the existing results. The query graph (G_q) awaits the arrival of a pattern where process P_2 writes the file Ff_1 . If so, a new node representing Ff_1 is added to the graph. According to the query graph, this $P \rightarrow Ff_1$ (write) is the desired one-hop attack path. For the above graph is $powershell.exe \rightarrow profile$ (write). Although in the query graph, $P \leftarrow Fg$ (read) occurs before $P \rightarrow Ff$ (write), since the previous operation read an ordinary file with weak attack relevance, if the provenance graph does not contain the corresponding related connected flow and nodes, it indicates that the operation did not introduce new suspicious attack semantics, and the next attack target should be further explored. Then, we search for the target

Algorithm 1 Threat Hunting Algorithm

Require: G_q, G_p
Ensure: Suspicious Subgraph G_s

```

1: /*DataProcessing*/
2:  $G_q \leftarrow MergeSimilarEntity(G_q)$ 
3:  $L_{Se} \leftarrow GetQuerySequences(G_q)$ 
4:  $f \leftarrow GetSetQueryGraphFlow(G_q)$ 
5:  $G_p \leftarrow MergeSimilarEvent(G_p)$ 
6: /*ThreatHunting and Incremental Aligning*/
7:  $FC \leftarrow FindCandidateNodes(G_q, G_p)$ 
8:  $relevant\_nodes \leftarrow ExtractRelevantNodes(G_q)$ 
9:  $attack\_sequence \leftarrow ReconstructAttackSequence(G_q)$ 
10:  $hunting\_sequence \leftarrow \emptyset$ 
11: for  $n \in relevant\_nodes$  do
12:    $context \leftarrow RetrieveNodeContext(n)$ 
13:    $hunting\_sequence.add(context)$ 
14: end for
15:  $hunting\_sequence.sort(key = \lambda x: x.timestamp)$ 
16:  $visited \leftarrow \emptyset$ 
17:  $fixed\_candidates \leftarrow \emptyset$ 
18:  $seqNum \leftarrow 0$ 
19: for  $context \in hunting\_sequence$  do
20:    $q\_node \leftarrow context.corresponding\_query\_node$ 
21:   if  $q\_node \notin visited$  then
22:      $candidates \leftarrow FC[q\_node]$ 
23:      $fixed\_candidates[q\_node] \leftarrow candidates$ 
24:      $visited[q\_node] \leftarrow True$ 
25:   else
26:      $candidates \leftarrow fixed\_candidates[q\_node]$ 
27:   end if
28:   for  $c \in candidates$  do
29:     if  $IsMaliciousSemantic(c)$  then
30:        $seqNum \leftarrow seqNum + 1$ 
31:        $node \leftarrow CreateTreeNode(c, seqNum)$ 
32:        $G_s.add(node)$ 
33:     end if
34:   end for
35: end for
36: return  $G_s$ 

```

corresponding to P→P (execute). In the P2 process node, there exists an execute action to another process P4 (the dashed line indicates no direct connection between nodes, and there are multiple hops), generating new tree nodes corresponding to P2. Similarly, in the newly added data on the right shaded part, there are interactions with sockets. As described above, the semantics represented by P6 are the same as those of P2, and the P2 node can be mapped to the P node in the query graph P→IP (connect), so P6→IP4 (connect) is equivalent to P2→IP4 (connect), allowing the generation of a new tree node.

V. EVALUATION

Our evaluation aims to answer the following five questions:

- **RQ1:** How effectively can ACTMINER detect the attacks especially in terms of false alarms?

TABLE IV: The detail of the attack and benign datasets.

Scenario	Behavior
E4-Trace case1	Malicious file download and execute
E4-Trace case2	Information gather and exfiltration
E4-Trace case3	Malicious file download and sensitive file exfiltration
E4-Trace case4	In-memory attack with firefox
E3-FiveDir case1	Pine backdoor
E3-FiveDir case2	Phishing E-mail Link with macro viruses
E3-Trace case1	Firefox backdoor and load malicious software
E3-Trace case2	Firefox backdoor and deploy malicious programme
E3-Trace case3	Phishing E-mail
E3-Theia case1	Firefox Backdoor and privilege escalation
Win Benign Data	Account operation, network communication and application activity
Linux Benign Data	User Login, application operation and network interaction

TABLE V: The summary of the experimental dataset. Column 1 specifies the name of dataset, and Column 2 denotes the corresponding duration. Columns 3 and 4 indicate the number of nodes and edges, respectively. Column 5 represents the number of attack nodes.

Datasets	Duration Time	# N	# E	% of Attack Nodes
E3-Trace	310h	1.950M	9.053M	37890
E3-FiveDirections	210h	1.287M	2.577M	2956
E3-THEIA	168h	960.357K	2.352M	14781
E4-Trace	8h	3.035M	13.586M	39582
Benign Linux	240h	2.385M	3.891M	0
Benign Windows	192h	5.324M	12.856M	0
Avg	234.667h	2.490M	7.386M	0.669%

- **RQ2:** How robust is ACTMINER against adversarial attacks?
- **RQ3:** How important are the components we design for assisting threat hunting?
- **RQ4:** How efficient is ACTMINER compared with the SOTA in terms of runtime overhead?
- **RQ5:** How robust is ACTMINER in benign dataset?

DataSet. ACTMINER is evaluated using three datasets: DARPA E3 [20], DARPA E4, Simulated Environments. The DarpaE3 dataset is open-source, whereas the DarpaE4 dataset is not publicly available. Theia and FiveDirections are both from DARPA Engagement 3, and Trace is from DARPA Engagement 3 and 4. The data of Theia and Trace was collected from the Linux, while the data of FiveDirections was collected from the Windows 7. As shown in Table V, the duration encompasses both benign activities and attack-related activities within a dataset, wherein only a small portion of the total time frame involves actual attacks. Detailed description of both actual attack behaviors and benign operations can be found in the Table IV.

As show in Table IV, these attacks include the following scenarios: malicious file downloads and execution, information collection and exfiltration, Firefox memory attacks, backdoor extensions, and phishing emails. Furthermore, we employ Kollect [34] to extract benign data from the Windows platform, while we utilize SPADE [38] for the acquisition of benign log data from Linux. All benign data includes various daily system operations, such as network browsing, file operations, etc. We also use the OpTC dataset which contains benign activities of 500 Windows hosts over seven days. These benign datasets contain billions of audit records on Windows, Linux, and FreeBSD.

Detector for Comparison. To evaluate ACTMINER, we use a graph alignment-based threat hunting system as benchmark: POIROT. **Why are we only comparing ACTMINER to**

POIROT? There are already several threat hunting studies [2], [11], [25], [39], [40]. We broadly categorise them into the following two based on the techniques they use: machine learning-based approaches [11], [39], [40] and search-based approaches [2], [25]. While both DeepHunter [39] and ProvG-Searcher [11] conduct model training by constructing positive (attack graphs extracted manually from the provenance graph) and crafted negative samples. MEGR-APT [40] utilizes a graph matching model to compute similarity scores between the query graph’s embedding vector and the embedding vectors of detected subgraphs. However, a fundamental limitation of these coarse-grained methods is their inability to consider the relationships between nodes in the attack chain (e.g., DeepHunter solely considers the relationships between IOCs rather than the comprehensive association information of all attack nodes). In other words, the results obtained from DeepHunter and ProvG-Searcher may not necessarily represent complete attack chains. Furthermore, our initial attempt to re-implement the ProvG-Searcher revealed that the core component responsible for processing both provenance graphs and query graphs is not available as an open-source solution. Hence, we do not compare our work with them. ThreatRaptor [25] uses NLP technology to extract threat behaviour graphs from CTI reports and transforms the graphs into TBQL query language using specific algorithms. Unlike ACTMINER, it stores audit log data in a database, allowing for the retrieval of individual attack behaviors. The single-point matching results obtained from the TBQL query statement do not correspond well to the contextual content of the attack process described in the CTI report. So we do not compare with it.

Here, we compare the performance of ACTMINER with POIROT [2], which are the most relevant in term of level and methodology for our evaluation. POIROT aligns the query graph with the provenance graph based on node type and name regularization. Due to the unavailability of the query graphs manually extracted by the authors in POIROT, for fairness, our query graph is uniformly extracted by the Extractor [28] in our experimental setting. However, during the extraction process, we encounter graph disconnections, incomplete attack chains, etc. Therefore, we use the state-of-the-art method CRUcialG [41] to assist in obtaining the query graph.

A. RQ1: How effectively can ACTMINER detect the attacks especially in terms of false alarms?

Table VI presents the performance of ACTMINER and POIROT on our evaluation datasets. ACTMINER consistently surpass POIROT, achieving superior precision, recall values and lower number of FN/FP. In comparison to POIROT, ACTMINER utilizes entities attributes and action semantic to generate a more generalizable query graph. This provides brief abstracted entity information to taking a graph alignment, subsequently reducing false negative and enhancing precision and recall. As the POIROT paper lacks evaluation on E4 dataset, we execute POIROT on E4 to obtain evaluation results. The findings demonstrate that ACTMINER significantly outperforms POIROT, as E4 attacks more challenging to detect due to well-blended malicious activity. POIROT relies solely

on name and simple types as query graph’s features, which is insufficient. On the other hand, the entities attributes and action semantic employed by ACTMINER offer more semantic information for each node and less sensitive for nodes with certain types of characteristics, making it harder for attack nodes to conceal themselves.

At first sight, ACTMINER shows incremental improvement in comparison to POIROT in terms of FN. This is attributed to ACTMINER considering the correlation between semantics of multi-hop nodes. Table VI shows the performance of ACTMINER and POIROT on all datasets. ACTMINER does not miss any malicious nodes, i.e., ACTMINER’s average false negatives (FNs) are 0, reduced by 61 compared to POIROT. On average, the false positive nodes generated by ACTMINER (~ 389 nodes) is $1.91 \times$ less than POIROT. ACTMINER demonstrates a notable improvement in precision over POIROT, achieving a 2.96% higher precision score, while also outperforming POIROT in terms of recall with a 1.94% increase.

B. RQ2: How robust is ACTMINER against adversarial attacks?

When an attack occurs, the attacker’s behavior pattern may be highly similar or even nearly identical to the normal system behavior in a regular environment. From a technical perspective, attackers can mimic normal processes at the API call level or employ code injection techniques to make their behavior patterns indistinguishable from normal processes at the low-level system log. This poses a challenge for provenance-based threat hunting. However, by considering richer contextual semantics, differentiation can still be achieved. Goyal et al. [42] devise three strategies for adversarial detection of anomaly detection systems based on graph-level granularity. Enlightened by their work, we design experiments to assess ACTMINER’s resilience against adversarial attacks.

To access ACTMINER’s resilience against adversarial attacks, we perform adversarial mimicry attacks on provenance-based graph alignment threat hunting system. To evaluate ACTMINER’s anti-attack capability, based on the Darpa datasets as a reference, we modify and add attack steps in the provenance graph, primarily considering two scenarios.

Scenario I: The attacker inserts a large number of invalid attack paths into the actual attack chain, attempting to disrupt and mislead the detection algorithm. Test results show that POIROT suffered severe missed detections in this scenario, while ACTMINER successfully detected all real attack nodes, resisting the attacker’s disruptive attacks.

Scenario II: The attacker uses normal programs to perform operations similar to attack patterns, attempting to introduce false positives. Tests found that the POIROT exhibits varying degrees of false positives, marking normal processes as attack nodes. Our system, on the other hand, effectively distinguishes the true intent of normal programs through behavior association and intent analysis, avoiding false positives. Based on the above two scenarios, we designed the following three strategies:

- 1) Strategy I: Insert additional unrelated benign process read/write file flows between process and file read/write operations. As shown in Figure 5;

TABLE VI: Performance of ACTMINER and POIROT. FN denotes the false negative, which occurs when a genuine attack pattern is incorrectly classified as benign. Conversely, FP represents the false positive, where a benign event or data point is mistakenly identified as an attack one. The notation Prec. denotes precision.

ATTACK	POIROT			ActMiner without EST			ActMiner		
	FN/FP	Recall	Prec.	FN/FP	Recall	Prec.	FN/FP	Recall	Prec.
Darpa4 Trace case1	19/89	99.79	99.00	21/43	99.76	99.51	0/79	100.00	99.11
Darpa4 Trace case2	58/1005	99.62	93.89	37/532	99.76	96.62	0/781	100.00	95.18
Darpa4 Trace case3	77/82	94.58	94.24	63/41	95.51	97.03	0/65	100.00	95.39
Darpa4 Trace case4	96/1352	98.51	88.61	74/775	99.30	93.16	0/912	100.00	92.15
Darpa3 FiveDir case1	18/254	98.52	82.49	7/88	99.42	93.19	0/142	100.00	89.40
Darpa3 FiveDir case2	49/49	96.36	96.36	32/30	97.59	97.74	0/37	100.00	97.32
Darpa3 Trace case1	77/1146	99.47	92.62	54/412	99.62	97.20	0/613	100.00	95.91
Darpa3 Trace case2	59/1952	99.67	90.20	35/742	99.80	95.95	0/996	100.00	94.80
Darpa3 Trace case3	78/233	94.72	85.72	62/103	95.76	93.14	0/154	100.00	90.08
Darpa3 Theia	85/1263	99.37	91.38	63/578	99.53	95.85	0/746	100.00	94.72
Avg FP/FN/Recall/prec.	61/742	98.06	91.45	45/334	98.60	95.94	0/452	100.00	94.41

† EST: Equivalent Semantic Transfer

- 2) Strategy II: Insert additional benign processes between process and process execution operations. As shown in Figure 6;
- 3) Strategy III: Insert additional processes communicating with sockets between processes and socket communication operations. As shown in Figure 7.

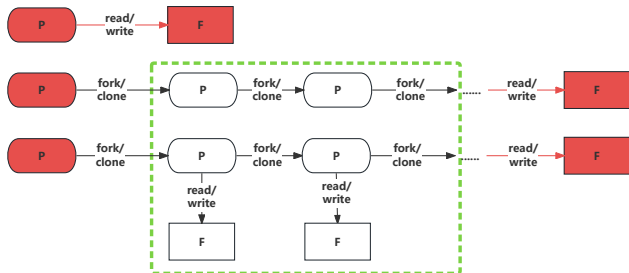


Fig. 5: Strategy I. Read/Write operations Insert.

The experimental results, as illustrated in Table VII, depict the percentage of nodes and edges incrementally added to the attack graph using the three aforementioned strategies on the Darpa 4 dataset across all attacks. Both nodes and edges are incrementally added at a constant rate.

In terms of recall rate, our system consistently maintains a high average ratio as the proportion of added nodes increases,

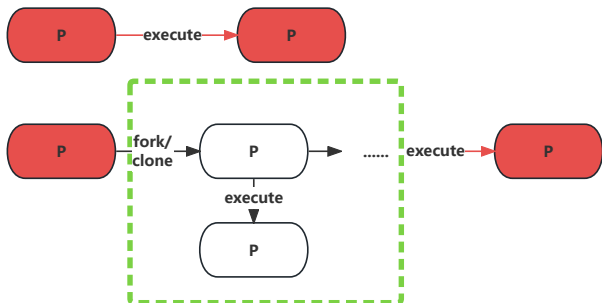


Fig. 6: Strategy II. Execute operations Insert.

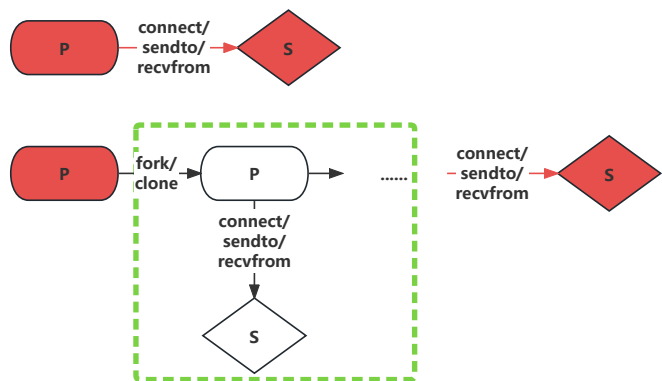


Fig. 7: Strategy III. Connect/Send/Recv operations Insert.

with a decreasing trend approaching approximately 1%. This characteristic is determined by the design of our system. In contrast, POIROT exhibits a diminishing recall rate as the proportion increases, with the rate of decline accelerating with higher proportions added. This can be observed from the AVG of R., where the descent shifts from an initial 1.5% at full scale to around 4% towards the latter end of the scale. Regarding precision, as the proportion increases, both our system and POIROT reach their respective lowest points of 89.33% and 69.75%. Through further analysis, we conclude that our system is capable of detecting evasion attacks based on the equivalent semantic approach we have devised.

Why can't POIROT defend against adversarial attacks?

The attacker inserts a large number of irrelevant nodes and connecting edges between the real attack steps, increasing the hop count of a single attack stage to more than three hops. This causes POIROT to fail to associate different stages as a single attack event, resulting in missed detection. POIROT decomposes the graph through bounded branches (γ) and depth (β), separating graph neighborhoods from each other. The authors of POIROT consider the optimal depth to be three. Therefore, even if suspicious nodes have a common malicious ancestor, if the hop distance of that behavior from the earliest attack node exceeds β hops, the anomaly score obtained by that behavior will be lower than the score of the previous malicious

TABLE VII: The performance comparison between the ACTMINER and POIROT across four scenarios (i.e., four query graphs) from the E4-Trace dataset, where varying proportions of edges and nodes are added in the provenance graph. Each addition consists of an equal number of three types of nodes/edges. The percentage added represents the percentage of the number of nodes in the provenance graph relative to the attack node.

Query Graph	0%				25%				50%			
	POIROT		ACTMINER		POIROT		ACTMINER		POIROT		ACTMINER	
	Precision	Recall	Precision	Recall	Precision	Recall	Precision	Recall	Precision	Recall	Precision	Recall
case1	99.00	99.79	100.00	100.00	98.34	99.23	100.00	100.00	96.24	97.35	99.26	100.00
case2	93.98	99.62	97.37	100.00	93.28	96.55	97.58	100.00	92.26	94.98	96.33	100.00
case3	94.24	94.58	98.32	100.00	93.21	94.52	98.42	100.00	91.35	92.25	96.47	100.00
case4	88.61	98.51	95.08	100.00	87.25	94.31	95.52	100.00	83.21	90.44	94.35	100.00
AVG	93.96	98.13	97.69	100.00	93.02	96.13	97.88	100.00	90.77	93.76	96.60	100.00
Query Graph	75%				100%				125%			
	POIROT		ACTMINER		POIROT		ACTMINER		POIROT		ACTMINER	
	Precision	Recall	Precision	Recall	Precision	Recall	Precision	Recall	Precision	Recall	Precision	Recall
case1	93.55	95.26	97.56	100.00	91.41	94.32	96.46	99.98	89.74	90.25	95.84	99.98
case2	90.04	93.52	94.32	100.00	87.43	90.78	94.16	100.00	82.36	87.32	92.52	99.98
case3	89.21	91.56	95.36	100.00	88.47	90.24	95.13	99.97	86.25	84.33	94.78	99.97
case4	80.32	87.03	93.42	100.00	77.22	85.41	92.74	100.00	74.32	81.36	92.04	99.97
AVG	88.28	91.84	95.17	100.00	86.13	90.19	94.62	99.99	83.17	85.82	93.80	99.98
Query Graph	150%				175%				200%			
	POIROT		ACTMINER		POIROT		ACTMINER		POIROT		ACTMINER	
	Precision	Recall	Precision	Recall	Precision	Recall	Precision	Recall	Precision	Recall	Precision	Recall
case1	87.21	88.41	92.36	99.98	82.34	81.64	91.50	99.96	77.28	76.88	90.03	98.74
case2	77.23	83.42	89.64	99.47	72.14	80.21	88.75	99.48	61.45	76.33	87.25	99.52
case3	83.52	81.02	93.74	99.86	79.42	77.31	92.36	99.23	75.04	73.98	91.11	99.13
case4	70.30	79.52	91.14	99.97	68.23	75.21	90.02	99.95	65.23	72.06	88.94	99.32
AVG	79.57	83.10	91.72	99.82	75.53	78.59	90.66	99.66	69.75	74.81	89.33	99.17

behavior, and that behavior may be mistaken as benign. The attacker can also insert a small number of irrelevant nodes between attack stages, keeping the hop number of the attack chain for each stage within POIROT’s detection threshold of three. Although the inserted nodes themselves are harmless, the edges connecting them to the real attack nodes cause POIROT to erroneously judge them as part of the attack, resulting in false negatives. Through our further investigation, we analyze the reasons behind the superior performance of ACTMINER: POIROT uses the query graph directly for regular matching of node types and their attribute names, and selects appropriate nodes based on path scores, neglecting to consider temporal and causal issues between nodes, resulting in many false alarms.

The robustness of ACTMINER results from two reasons. First of all, during the construction of suspicious semantic tree, attack intent information would be confirmed. The asserted behaviors like fork/clone will not influence the score of the certain attack path, because the multiple-hops strategy will consider these nodes to contain the same suspicious semantic. Second, ACTMINER do not raise alarms unless nodes exceeding the attack sequence length are detected. This ensures that our system does not generate excessive false positives when attackers intend to conduct multi-point blasting to affect the hunting system, while also enhancing its resilience against Scenario I.

C. RQ3: How important are the components we design for assisting threat hunting?

To demonstrate the impact of our system components, particularly the query graph processing (QGP) and equivalent semantic transfer (EST) components on system performance

and efficiency, we conduct ablation experiments on them separately. The QGP step is responsible for generating the required query graphs, and facilitating the subsequent operations of our system. On the other hand, the EST step plays a crucial role in threat hunting module.

1) **Efficacy of Equivalent Semantic Transfer.** We test the performance of ACTMINER without EST using the same settings in the RQ1. As demonstrated in Table VI, without the EST component the number of FN enhanced by 1.4%, the number of false positives is 83.96% of POIROT’s, while it represented an increase compared to ACTMINER. It is attributed to the following reasons: The process of equivalent semantic transfer also inherently involves the causal logic and temporal relationships of the attack to some extent. Therefore, removing this component may introduce a small portion of false positives.

2) **Effectiveness of Query Graph Processing.** As part of our study, we directly utilize the query graphs extracted by the Extractor and CRUcialG on the same provenance graphs used in RQ1 for threat hunting. The size of query graph before QGP and after QGP for all situations are presented in Table VIII, along with the results and the corresponding analysis. In the QGP process, we uses the method of attribute abstraction for nodes, so the number of nodes would be reduced. Our analysis explores the impact of incorporating Query Graph Processing (QGP) on the system’s accuracy and timeliness. We use the Trace dataset from E3 to study the effect of QGP. The result, presented in Figure 8, shows a significant reduction in time consumption when considering QGP. This improvement results from QGP further merging the extracted nodes. Ignoring query graph processing makes efficiently hunting these nodes challenging. However, incorporating QGP allows the system

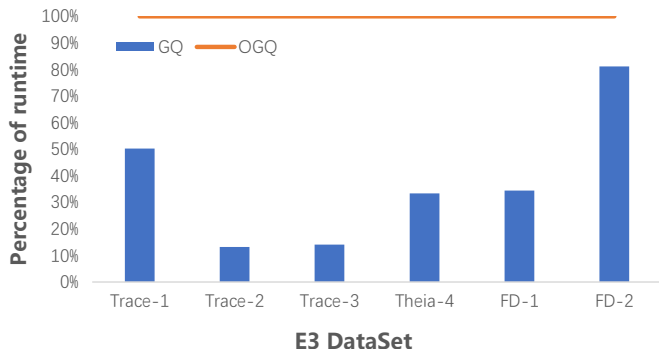


Fig. 8: Ratio of running time between GQ and OGQ. OGQ denotes the original query graph, the GQ denotes the query graphs we use in ACTMINER.

TABLE VIII: The edges and nodes in the query graph, OV and OE denote the number of nodes and edges in the graph before QGP, and V and E denote the number of nodes and edges after processing, respectively.

Scenario	E4				E3						
	T-1	T-2	T-3	T-4	Tr-1	Tr-2	Tr-3	Th-1	W-1	W-2	
OV	9	13	16	9	14	10	15	12	13	10	
OE	8	13	17	8	16	11	14	14	14	11	
V	6	4	6	8	6	8	5	6	5	7	
E	6	3	5	7	5	9	4	5	4	6	

to identify these nodes more effectively, leading to improved threat hunting performance.

D. RQ4: How efficient is ACTMINER compared with the SOTA in terms of runtime overhead?

We evaluate how efficiently ACTMINER can detect APT attacks in a timely manner by measuring its running time performance. As shown in Table IX, it can be seen that under the overall time overhead, POIROT consumes 1.69 times more time than ACTMINER. This suggests that ACTMINER has better timeliness compared to POIROT. However, in some cases, especially the scenario of E3-Trace case1. Through our further investigation, we have discovered a key cause that led to this discrepancy. ACTMINER employs a mechanism to offload data instances spanning over 6 hours from memory to the database. While beneficial for optimizing memory management, this storage approach incurs extra overhead when encountering situations that necessitate repeated interactions between the database and memory, resulting in higher time expenditure compared to POIROT.

Furthermore, the presence of an incremental hunting module allows our system to input data in segments for hunting, rather than having to input all the data at once for each hunt. Specifically, enterprises only need to input the newly added data to the system for each batch (e.g., the data from each day), instead of combining it with data from previous days and performing rescanning. At the same time, we have designed a storage mechanism that stores branches in a database. When an edge interacting with that node appears again, the branch is retrieved from the database.

Instead of loading all historical data for each new hunt, only the newly collected information needs to be processed

TABLE IX: Overhead of ACTMINER and POIROT.

ATTACK	POIROT			ActMiner		
	Ti.(s)	Mem.(MB)	CPU(%)	Ti.(s)	Mem.(MB)	CPU(%)
E4-Trace case1	2931	65.2	28.3	5	86.6	25.7
E4-Trace case2	2311	95.6	28.6	82	118.1	25.7
E4-Trace case3	102	27.8	26.4	28	35.8	26.0
E4-Trace case4	4284	69.4	28.3	69	105	25.7
E3-FiveDir case1	5	53.5	26	26	46.2	21.4
E3-FiveDir case2	73	31.0	29	6	50.2	23.7
E3-Trace case1	7814	178.1	26.5	15927	112	27.2
E3-Trace case2	39701	348.8	25.5	9982	155.4	25.4
E3-Trace case3	62	27.8	25	149	55.9	25.5
E3-Theia	3416	280.3	26.8	9629	105.3	25.0
Avg	6070	117.8	27.1	3590	87.1	25.1

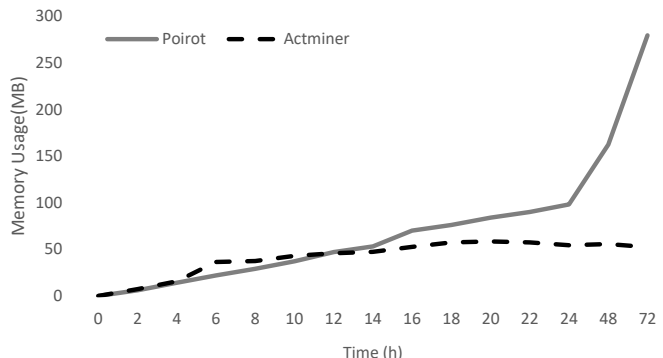


Fig. 9: Average Memory consumption in different time states.

and indexed. As illustrated in the Figure 9, POIROT’s mean memory requirements gradually increase as more data is collected from hosts over time. However, our incremental hunting module ensures that the rate of memory consumption growth is consistently maintained at a steady pace, primarily determined by our storage mechanism.

E. RQ5: How robust is ACTMINER in benign dataset?

To comprehensively evaluate the robustness of ACTMINER, we conducted experiments on a sizeable benign dataset, introduced in Section V. This dataset was collected from multiple users performing typical non-malicious actions such as downloading and uploading files, taking backups, browsing the web, and installing or uninstalling software. Additionally, we included the OpTC dataset, which involves benign activities like website browsing, checking emails, and SSH log-ins. We randomly selected three hosts and tested their benign data collected over a period of one day from the OpTC dataset and five datasets acquired from our own laboratory.

We applied ACTMINER to all benign datasets and searched for the query graphs extracted from the TC reports. Although these logs were attack-free, they shared many nodes and processes related to email clients and text editing tools. As illustrated in Table X, despite these similarities, ACTMINER successfully demonstrated robustness by generating zero false alerts throughout the experiment.

VI. DISCUSSION & FUTURE WORK

The accuracy of ACTMINER. Due to the accuracy of threat hunting relying on the quality of query graphs, we utilized EXTRACTOR to automate the extraction of CTI

TABLE X: Experimental results on different benign datasets.

DataSet	Test Duration	Platform	Hosts	FP
OpTC	01d00h00m	Window	3	0
Our Lab	01d08h13m	Ubuntu 12.04 x64	5	0

reports provided by DARPA. We achieved results superior to the SOTA on well-known APT attack datasets (i.e., E3 and E4). However, limited by scarce APT attack samples, we were unable to conduct large-scale experiments and analyses. In practice, accurately extracting query graphs from numerous CTI reports and automatically generating diverse and rational ones can improve threat hunting accuracy in the future.

The interpretability of ACTMINER. The outputs of ACTMINER inherently provide interpretability, as analysts can derive attack-related information from the query graphs reports. However, due to the dynamic nature of APT attacks, the query graphs and hunting results are not entirely consistent. Therefore, in the future, we can utilize generative artificial intelligence (e.g., LLM), to automatically transform the attack chains obtained from threat hunting into CTI reports that analysts can clearly understand, aiding in better response.

The robustness of ACTMINER. The use of graph processing approaches may lead to the loss of fine-grained details. To validate the robustness of our ACTMINER, we conducted cross-validation by employing query graphs extracted from diverse CTI reports against distinct provenance graphs. The experimental findings consistently demonstrate that our system effectively avoids generating false alarms across all tested origin query graphs. The identified suspicious nodes do not meet the threshold for triggering an alert.

VII. RELATEDWORK

A. Provenance Graph-based Threat Hunting

The provenance graph contains causal relationships between system events, and it is a data structure that can be effectively utilized for cyber threat hunting. DeepHunter [39] utilizes Neural Tensor Networks (NTN) to judge the subgraph relationship through graph embedding. Due to the need for multiple-to-multiple traversal comparisons between subgraphs, the efficiency of DeepHunter will decrease as the size of the provenance graph increases. ProvG-Searcher [11] establishes a coarse-grained threat hunting by employing a graph representation learning method on the subgraph, aiming to enhance hunting efficiency. ThreatRaptor [25] achieves extracting structured threat behaviors from OSCTI and automatically synthesizing query statements to search for malicious activities. Unlike the above studies, ACTMINER, inspired by POIROT [2], tries to align attack graphs extracted from CTI reports with provenance graphs from system logs to find complete attack chain. However, ACTMINER is able to significantly reduce false positives, false negatives, and system overhead through an optimized graph alignment algorithm.

B. Graph Matching Algorithms

Graph pattern matching refers to the problem of finding similarities between a small query graph and a large target graph,

with widespread applications (e.g., database analysis, search engines, software plagiarism detection, and social networks). Based on whether the matching results are completely consistent, algorithms can be divided into two categories: graph isomorphism matching and graph approximate matching. The main idea of graph isomorphism matching algorithms is to iteratively map nodes from the query graph to the target graph one by one. Ullmann et al. [43] proposes a backtracking-based algorithm that enumerates all subgraphs satisfying the matching requirements using a depth-first search approach. However, as the scale of the graph gradually increases, the enumeration range also expands, resulting in low algorithm efficiency. To address this issue, Cordella et al. [44] proposes the VF2 algorithm, which improves algorithm efficiency by incorporating the verification order of query nodes. However, in practical applications, its time complexity is superlinear, and the need for secondary filtering consumes a significant amount of time. Shasha et al. [45] introduces the GraphGrep algorithm, which achieves fast matching by encoding node semantic information. Several other studies [46]–[48] use graph mining techniques to find subgraphs from databases and then employ filtering and optimization strategies to prune incorrect nodes. However, due to the diversity and complexity of APT techniques, we cannot always assume that the nodes and edges of the query graph can be fully mapped to the target graph. Graph approximate matching algorithms often rely on heuristic methods to identify important nodes and then gradually expand to neighboring nodes [2], [49]–[51]. Tian et al. [49] uses a graph distance model to measure the similarity between graphs. He et al. [52] introduces an index-based algorithm to support subgraph queries and similarity queries. Several other works [51], [53] consider the shape and edge attributes of the query graph. However, the aforementioned research overlooks adversarial knowledge. Milajerdi et al. [2] proposes POIROT, which is similar to our work and utilizes node attributes and information flows between nodes for approximate matching. However, if an attacker intentionally takes a detour to achieve their goal, it may result in missed detections. Furthermore, if the similarity score exceeds the threshold, POIROT stops hunting, and the obtained attack subgraph may not represent the optimal attack behavior. Therefore, we develop a new matching technique to address these challenges.

C. Incremental Graph Computation

In real-world scenarios, graphs are typically large in scale and frequently updated over time. When graphs are updated, traditional batch processing methods require starting the computation from scratch, which is extremely time-consuming. In contrast to traditional batch processing algorithms, incremental matching only analyzes and matches the updated portion, utilizing previous matching results to maximize the reduction of redundant computations. Fan et al. proposes the IncSIMMatch [54] algorithm, which effectively reduces redundant computations by creating an index for the pattern graph. They then introduce an incremental computation method IncISO [55], where only the set of nodes within d hops of the updated node d in the data graph needs to be rematched as the affected region

when nodes and edges change in the graph. Subsequently, researchers [56]–[62] introduce the idea of incremental computation and incorporated query search optimization strategies. For example, Sutanay et al. [57] constructs the pattern graph as a binary tree and decomposes it for storage in tree nodes, with data updates performed by searching leaf nodes. However, storing a large number of indexes consumes memory. Sun et al. [63] proposes an exploration-based approximate matching technique, but if the initially selected node is inappropriate, a large number of useless intermediate result values will be generated. ACTMINER constructs a tree structure to incrementally update the alignment results and introduces a forgetting rate to maintain stable memory overhead.

VIII. CONCLUSION

We propose ACTMINER, a system that enables the detection of the complete APT attacks chains by applying causality tracking and increment aligning. It overcomes the issues of low precision, low recall, and low efficiency that existed in previous work. Experimental results show that ACTMINER exhibits better detection rates and resilience against adversarial attacks compared to the SOTA.

REFERENCES

- [1] A. Bates *et al.*, “Trustworthy {Whole-System} provenance for the linux kernel,” in *USENIX*, 2015, pp. 319–334.
- [2] S. M. Milajerdi *et al.*, “Poivot: Aligning attack behavior with kernel audit records for cyber threat hunting,” in *CCS*, 2019, pp. 1795–1812.
- [3] Milajerdi, Sadegh M and others, “Holmes: real-time apt detection through correlation of suspicious information flows,” in *S&P*. IEEE, 2019, pp. 1137–1152.
- [4] M. N. Hossain *et al.*, “Combating dependence explosion in forensic analysis using alternative tag propagation semantics,” in *S&P*. IEEE, 2020, pp. 1139–1155.
- [5] Y. Xie *et al.*, “Pagoda: A hybrid approach to enable efficient real-time provenance based intrusion detection in big data environments,” *TDSC*, 2018.
- [6] M. Bishop *et al.*, *Introduction to computer security*. Addison-Wesley Boston, 2005, vol. 50.
- [7] C. Kruegel *et al.*, *Intrusion detection and correlation: challenges and solutions*. Springer Science & Business Media, 2004, vol. 14.
- [8] C. Xiong *et al.*, “Conan: A practical real-time apt detection system with high accuracy and efficiency,” *TDSC*, 2020.
- [9] T. Zhu *et al.*, “Aptshield: A stable, efficient and real-time apt detection system for linux hosts,” *TDSC*, 2023.
- [10] M. N. Hossain *et al.*, “{SLEUTH}: Real-time attack scenario reconstruction from {COTS} audit data,” in *USENIX*, 2017.
- [11] E. Altinisik *et al.*, “Provg-searcher: A graph representation learning approach for efficient provenance graph search,” in *CCS*, 2023.
- [12] J. Zengy *et al.*, “Shadewatcher: Recommendation-guided cyber threat analysis using system audit records,” in *S&P*. IEEE, 2022.
- [13] S. Wang *et al.*, “Threatrace: Detecting and tracing host-based threats in node level through provenance graph learning,” *TIFS*, vol. 17, pp. 3972–3987, 2022.
- [14] X. Han, *et al.*, “Unicorn: Runtime provenance-based detector for advanced persistent threats,” pp. 1–18, 2020.
- [15] E. Manzoor *et al.*, “Fast memory-efficient anomaly detection in streaming heterogeneous graphs,” in *Dblp*, 2016, pp. 1035–1044.
- [16] M. U. Rehman *et al.*, “Flash: A comprehensive approach to intrusion detection via provenance graph representation learning,” in *S&P*. IEEE, 2024, pp. 139–139.
- [17] F. Yang *et al.*, “{PROGRAPHER}: An anomaly detection system based on provenance graph embedding,” in *USENIX*, 2023, pp. 4355–4372.
- [18] “Threat report,” <https://www.crowdstrike.com/global-threat-report/>.
- [19] “Lateral movement,” <https://www.crowdstrike.com/cybersecurity-101/lateral-movement/>.
- [20] A. D. Keromytis., “Transparent computing engagement 3 data release.” 2018, <https://github.com/darpa-i2o/Transparent-Computing/blob/master/README-E3.md>.
- [21] “Darpa transparent computing engagement,” 2020, <https://www.darpa.mil/program/transparent-computing>.
- [22] “mandiant/openioc_1.1.,” <https://github.com/mandiant/OpenIOC/>.
- [23] “Introduction to stix,” <https://oasis-open.github.io/cti-documentation/stix/intro.html>.
- [24] “Misp - open source threat intelligence platform & open standards for threat information sharing,” <https://www.misp-project.org>.
- [25] P. Gao *et al.*, “Enabling efficient cyber threat hunting with cyber threat intelligence,” in *ICDE*. IEEE, 2021, pp. 193–204.
- [26] G. Husari *et al.*, “Ttpdrill: Automatic and accurate extraction of threat actions from unstructured text of cti sources,” in *ACSAC*, 2017.
- [27] X. Liao *et al.*, “Acing the ioc game: Toward automatic discovery and analysis of open-source cyber threat intelligence,” in *CCS*, 2016.
- [28] K. Satvat *et al.*, “Extractor: Extracting attack behavior from threat reports,” in *EuroS&P*. IEEE, 2021, pp. 598–615.
- [29] W. U. Hassan *et al.*, “Nodoze: Combatting threat alert fatigue with automated provenance triage,” in *NDSS*, 2019.
- [30] Hassan, Wajih Ul and others, “Tactical provenance analysis for endpoint detection and response systems,” in *S&P*. IEEE, 2020, pp. 1172–1189.
- [31] Q. Wang *et al.*, “You are what you do: Hunting stealthy malware via data provenance analysis,” in *NDSS*, 2020.
- [32] Inam, Muhammad Adil and others, “Sok: History is a vast early warning system: Auditing the provenance of system intrusions,” in *S&P*. IEEE, 2023, pp. 2620–2638.
- [33] R. Sekar *et al.*, “eaudit: A fast, scalable and deployable audit data collection system,” in *S&P*. IEEE, 2023, pp. 87–87.
- [34] T. Chen *et al.*, “Kollect: a kernel-based efficient and lossless event log collector,” *arXiv preprint arXiv:2207.11530*, 2022.
- [35] “Windows event tracing,” <https://docs.microsoft.com/en-us/windows/desktop/ETW/event-tracing-portal/>. [Online]. Available: <https://docs.microsoft.com/en-us/windows/desktop/ETW/event-tracing-portal/>
- [36] T. Zhu *et al.*, “General, efficient, and real-time data compaction strategy for apt forensic analysis,” *TIFS*, vol. 16, pp. 3312–3325, 2021.
- [37] “Darpa3-cdm.” [Online]. Available: <https://drive.google.com/drive/folders/1gwm2gAlKHQnFvETgPA8KJXLm3L-Z3H1>
- [38] A. Gehani *et al.*, “Spade: Support for provenance auditing in distributed environments,” in *Middleware 2012: ACM/IFIP/USENIX 13th International Middleware Conference, Montreal, QC, Canada, December 3-7, 2012. Proceedings 13*. Springer, 2012, pp. 101–120.
- [39] R. Wei *et al.*, “Deephunter: A graph neural network based approach for robust cyber threat hunting,” in *SecureComm*. Springer, 2021, pp. 3–24.
- [40] A. Aly, S. Iqbal, A. Youssef, and E. Mansour, “Megr-apt: A memory-efficient apt hunting system based on attack representation learning,” *IEEE Transactions on Information Forensics and Security*, vol. 19, pp. 5257–5271, 2024.
- [41] W. Cheng, T. Zhu, T. Chen, Q. Yuan, J. Ying, H. Li, C. Xiong, M. Li, M. Lv, and Y. Chen, “Crucialg: Reconstruct integrated attack scenario graphs by cyber threat intelligence reports,” *arXiv preprint arXiv:2410.11209*, 2024.
- [42] A. Goyal *et al.*, “Sometimes, you aren’t what you do: Mimicry attacks against provenance graph host intrusion detection systems,” in *NDSS*, 2023.
- [43] J. R. Ullmann, “An algorithm for subgraph isomorphism,” *JACM*, vol. 23, no. 1, pp. 31–42, 1976.
- [44] L. P. Cordella *et al.*, “A (sub) graph isomorphism algorithm for matching large graphs,” *IEEE Trans. Pattern Anal. Mach. Intell.*, vol. 26, no. 10, pp. 1367–1372, 2004.
- [45] D. Shasha *et al.*, “Algorithmics and applications of tree and graph searching,” in *PODS*, 2002, pp. 39–52.
- [46] J. Cheng *et al.*, “Fg-index: towards verification-free query processing on graph databases,” in *SIGMOD*, 2007, pp. 857–872.
- [47] P. Zhao *et al.*, “Graph indexing: tree+delta= graph,” in *VLDB*. Citeseer, 2007, pp. 938–949.
- [48] X. Yan *et al.*, “Graph indexing: a frequent structure-based approach,” in *SIGMOD*, 2004, pp. 335–346.
- [49] Y. Tian *et al.*, “Saga: a subgraph matching tool for biological graphs,” *Bioinformatics*, vol. 23, no. 2, pp. 232–239, 2007.
- [50] Tian, Yuanyuan and others, “Tale: A tool for approximate large graph matching,” in *ICDE*. IEEE, 2008, pp. 963–972.
- [51] H. Tong *et al.*, “Fast best-effort pattern matching in large attributed graphs,” in *Proceedings of the 13th ACM SIGKDD international conference on Knowledge discovery and data mining*, 2007, pp. 737–746.
- [52] H. He *et al.*, “Closure-tree: An index structure for graph queries,” in *ICDE*. IEEE, 2006, pp. 38–38.

- [53] D. J. Pohly *et al.*, “Hi-fi: collecting high-fidelity whole-system provenance,” in *ACSAC*, 2012, pp. 259–268.
- [54] W. Fan *et al.*, “Incremental graph pattern matching,” *TODS*, vol. 38, no. 3, pp. 1–47, 2013.
- [55] Fan, Wenfei and others, “Incremental graph computations: Doable and undoable,” in *SIGMOD*, 2017, pp. 155–169.
- [56] J.-S. Kao and others, “Distributed incremental pattern matching on streaming graphs,” in *HPGP*, 2016, pp. 43–50.
- [57] S. Choudhury *et al.*, “A selectivity based approach to continuous pattern detection in streaming graphs,” *arXiv preprint arXiv:1503.00849*, 2015.
- [58] C. Kankanamge *et al.*, “Graphflow: An active graph database,” in *SIGMOD*, 2017, pp. 1695–1698.
- [59] M. Idris *et al.*, “The dynamic yannakakis algorithm: Compact and efficient query processing under updates,” in *SIGMOD*, 2017.
- [60] Idris, Muhammad and others, “General dynamic yannakakis: conjunctive queries with theta joins under updates,” *The VLDB Journal*, vol. 29, no. 2-3, pp. 619–653, 2020.
- [61] K. Kim *et al.*, “Turboflux: A fast continuous subgraph matching system for streaming graph data,” in *SIGMOD*, 2018, pp. 411–426.
- [62] S. Min *et al.*, “Symmetric continuous subgraph matching with bidirectional dynamic programming,” *arXiv preprint arXiv:2104.00886*, 2021.
- [63] X. Sun *et al.*, “An in-depth study of continuous subgraph matching,” *Proceedings of the VLDB Endowment*, pp. 1403–1416, 2022.